Caspase recruitment domain protein 6 is a microtubule-interacting protein that positively modulates NF-κB activation

Almut Dufner*, Scott Pownall[†‡], and Tak W. Mak*[†§]

*Campbell Family Institute for Breast Cancer Research, Toronto, ON, Canada M5G 2C1; and [†]Ontario Cancer Institute, Toronto, ON, Canada M5G 2C1

Contributed by Tak W. Mak, December 1, 2005

Proteins containing a caspase recruitment domain (CARD) play pivotal roles in signal transduction leading to apoptosis and NF-κB activation and inflammation. Here we identify and characterize human and mouse CARD protein 6 (CARD6), CARD-containing proteins of unique structure. CARD6 associates with microtubules and interacts with receptor-interacting protein (RIP)-like interacting caspase-like apoptosis regulatory protein kinase (RICK), a CARD-containing member of the RIP family of protein kinases. These kinases are involved in multiple NF-κB signaling pathways important for innate and adaptive immune responses. Surprisingly, the CARDs of CARD6 and RICK were not required for their interaction; instead, mutational analysis revealed that the CARD of CARD6 negatively controls the association of these molecules. CARD6 also binds to RIP1, a RIP kinase homologue that lacks a CARD but contains a C-terminal death domain. Coexpression of RICK targets CARD6 to aggresomes via a mechanism that requires the CARD of RICK. Importantly, CARD6 expression has a synergistic effect on NF-κB activation induced by several independent signal transduction pathways. In summary, our results indicate that CARD6 is a regulator of NF-κB activation that modulates the functions of RIP kinase family members.

signal transduction | immunity | receptor-interacting protein kinases

The regulation of many genes involved in immune responses, cell proliferation, and apoptosis is mediated by the inducible transcription factor NF-κB (1). These cellular processes are also controlled by proteins containing a caspase recruitment domain (CARD) (2). The CARD comprises an antiparallel six-helical bundle that mediates homotypic protein–protein interactions (3). In this study, we have identified and characterized CARD protein 6 (CARD6), a CARD protein of unique structure. Stehlik *et al.* (4) have reported a 311-aa variant of 1,037-aa human CARD6 that we refer to as CINCIN1 [CARD-containing inhibitor of nucleotide-binding oligomerization domain (NOD)1 and CARD-containing IL-1β converting enzyme (ICE) associated kinase (CARDIAK)-induced NF-κB activation; GenBank accession no. AY196783] (4).

Most signal transduction pathways that lead to NF-κB activation depend on the activation of receptor-interacting protein (RIP) kinases. RICK (also known as CARDIAK and RIP2) is a CARD-containing RIP kinase (5–7) that is essential for NF-κB activation triggered by NOD proteins (8–10). NOD proteins are CARD- and leucine-rich repeat (LRR)-containing Apaf-1-like molecules that transduce NF-κB activation in response to the recognition of intracellular bacterial peptidoglycan by the LRR (11–14). Gene ablation studies in mice have shown that RICK is also required for efficient signaling initiated by IL-1, IL-18, or the engagement of Toll-like receptors (TLR)2, -3, and -4 (9, 10). Moreover, RICK function is critical for optimal antigen-induced B cell lymphoma/leukemia 10 (BCL10)-dependent NF-κB activation in T cells (9, 15). RIP1, -3, and -4 are additional RIP kinase family members that regulate NF-κB activation (16). These enzymes have similar N-terminal kinase domains but differ in their C termini. In contrast to RICK, which has a CARD at its C terminus, RIP1 possesses a death domain. RIP1 mediates NF-κB activation induced by DNA damage (17) or by engagement of TNF receptor 1 (18, 19) or TLR3 (20). RIP1 is also involved in intracellular double-stranded RNA-activated type I IFN expression (21).

Although it is clear that RIP kinases control NF-κB activation triggered by multiple signaling pathways, the precise roles of these enzymes remain undefined. In this study, we demonstrate that the CARD protein CARD6 is a microtubule-associated protein that forms complexes with both RICK and RIP1. Our results indicate that CARD6 is a RIP kinase-interacting protein that positively modulates signal transduction pathways converging on NF-κB activation.

Results

Identification of CARD6. In a profile search for novel human CARD-containing molecules (see *Supporting Text*, which is published as supporting information on the PNAS web site), we identified a 1,037-aa CARD protein of unique structure that contains the CARD at the N terminus, a glutamic acid-rich region (GARR) following the CARD, and a proline-rich region (PRR) at the C terminus (Fig. 6*A*, which is published as supporting information on the PNAS web site). The human cDNA was recently deposited in GenBank under the name CARD6 (GenBank accession no. AF356193). We were able to clone both the predicted human and mouse (GenBank accession no. XM_139295) cDNAs. The CARD was most homologous to the CARD of the 208-aa Apoptosis Repressor with CARD protein (22). Moreover, amino acids 317–665 of human CARD6 exhibited 48% similarity to up-regulated gene 4 (URG4) (Fig. 6*A*, URG4 homology region), a growth and survival factor up-regulated in response to Hepatitis Bx antigen overexpression (23). CINCIN1 possesses the CARD6 CARD and GARR but does not include the adjacent C-terminal region containing the URG4 homology region and the PRR. Rather, the C-terminal region of CINCIN1 is derived from a distinct 3′-terminal exon that has its own polyA signal and encodes 30 amino acids that lack homology to CARD6 (Fig. 6*B*).

Northern blotting revealed that the human CARD6 transcript of 4.2 kb was expressed in most tissues examined (Fig. 7*A*, which is published as supporting information on the PNAS web site). The mouse CARD6 transcript was most highly expressed in spleen, liver, and testis.

We generated expression vectors encoding FLAG-tagged

Conflict of interest statement: No conflicts declared.

Freely available online through the PNAS open access option.

Abbreviations: CARD, caspase recruitment domain; NOD, nucleotide-binding oligomerization domain; GARR, glutamic acid-rich region; kd, kinase-dead; PRR, proline-rich region; RIP, receptor-interacting protein; siRNA, small interfering RNA; TLR, Toll-like receptor; URG4, up-regulated gene 4; HA, hemagglutinin; HEK, human embryonic kidney; RICK, RIP-like interacting caspase-like apoptosis regulatory protein kinase; CINCIN1, CARD-containing inhibitor of NOD1 and CARD-containing IL-1β converting enzyme-associated kinase-induced NF-κB activation; BCL, B cell lymphoma/leukemia.

[‡]Present address: enGene, Inc., 2386 East Mall, Suite 100, Vancouver, BC, Canada V6T 1Z3.

[§]To whom correspondence should be addressed. E-mail: tmak@uhnres.utoronto.ca.

www.pnas.org/cgi/doi/10.1073/pnas.0510380103

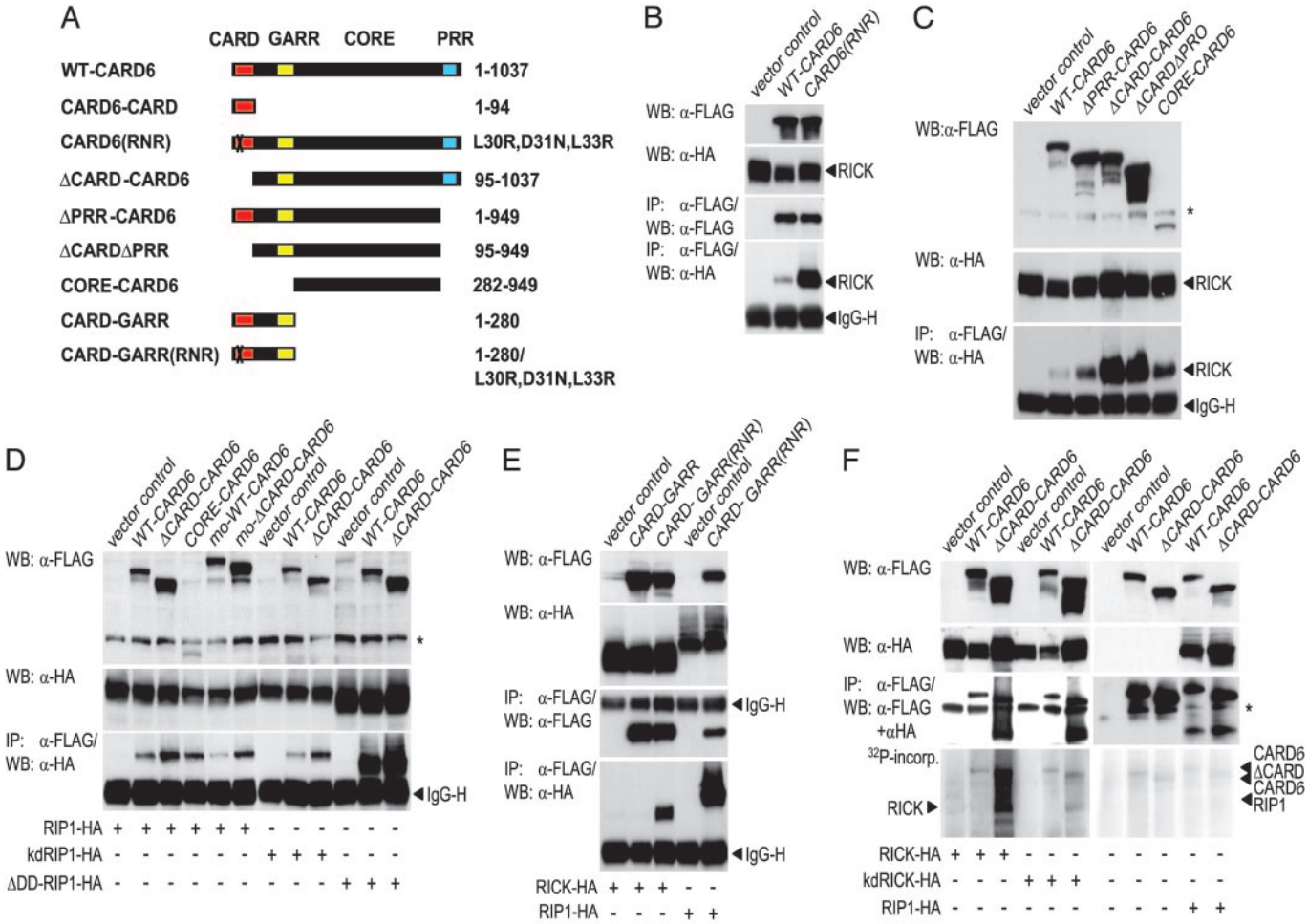

Fig. 1. Interaction of CARD6 with RICK and RIP1. (*A*) Mutated CARD6 expression constructs. Numbers identify the position of the indicated residues in the native human CARD6 protein. In the CARD6(RNR) mutant, three amino acid residues of the CARD essential for CARD–CARD interactions (X) are mutated (L30R, D31N, and L33R). All proteins were expressed as fusion proteins with a C-terminal FLAG-tag except for CARD6-CARD, which contains a C-terminal HA-tag. (*B–F*) HEK293T cells were transfected with empty vector or the indicated FLAG-tagged CARD6 constructs (*Top*) plus HA-tagged RICK (*B* and *C*) or the HA-tagged RIP1 and RICK constructs indicated at the bottom of *D–F*. Cell lysates were immunoprecipitated with anti-FLAG Ab and immunoblotted with anti-HA(3F10) Ab (and anti-FLAG Ab, where indicated). Fractions of the input were immunoblotted with anti-FLAG (*Top*) or anti-HA(3F10) Ab (second from top). In *F*, immunoprecipitations were subjected to a kinase assay before Western blotting (WB). *F Bottom* shows an autoradiograph of the WB that was scanned before quantification of the HA- and FLAG-tagged proteins in the pulldown with anti-HA(3F10) and anti-FLAG Abs (third panel from top). Results for each experiment are representative of at least three independent trials. WB, Western blot; IP, immunoprecipitation; IgG-H, IgG heavy chain; *, crossreactive band.

human WT-CARD6 and various truncation mutants lacking the CARD, PRR, or combinations of the CARD, PRR, and GARR (Fig. 1*A*). In addition, we generated the CARD6(RNR) and CARD-GARR(RNR)-CARD6 mutants in which three residues essential for homophilic CARD–CARD interactions were altered (Fig. 7*B*). In contrast to WT-CARD6, CARD6(RNR) did not bind to a hemagglutinin (HA)-tagged CARD6 truncation mutant that contained only the CARD (Fig. 7*C*).

CARD6 Interacts with RICK and RIP1. To determine CARD6 function, we performed a series of coimmunoprecipitation experiments involving FLAG-tagged WT-CARD6 and CARD6(RNR) tested against various HA-tagged CARD-containing proteins overexpressed in human embryonic kidney (HEK)293T cells. This approach led to the identification of RICK as a CARD6-interacting protein (Fig. 1*B*). Unexpectedly, RICK bound more strongly to CARD6(RNR) than to WT-CARD6, indicating that the interaction of these two CARD-containing molecules is not mediated by their CARDs. Accordingly, removal of the CARD from CARD6 (ΔCARD-CARD6) did not diminish RICK binding to CARD6 (Fig. 1*C* and Fig. 8*A*, which is published as supporting information on the PNAS web site). Indeed, CORE-CARD6 (amino acids 282–949) proved sufficient for RICK binding (Fig. 1*C*). Conversely, examination of the binding of RICK truncation mutants showed that the CARD of RICK was neither required nor sufficient for its association with ΔCARD-CARD6 (Fig. 8*B*); neither could we detect binding of the RICK-CARD or ΔCARD-RICK to WT-CARD6. RICK kinase activity was not critical for CARD6–RICK interaction (Fig. 8*C*). Mouse ΔCARD-CARD6 also bound to human (Fig. 8*D*) and mouse RICK (data not shown). However, we could not detect any binding of mouse WT-CARD6 to RICK. Taken together, these data suggest that the core region of CARD6 mediates binding to RICK in a manner that is negatively affected by the CARD of CARD6.

To determine whether CARD6 interacted with other RIP kinases, we tested whether human or mouse CARD6 could associate with RIP1. RIP1 was indeed pulled down by WT-CARD6 and ΔCARD-CARD6 of both species, but in contrast to RICK, this interaction was not significantly affected by the CARD (Fig. 1*D*). The interaction between RIP1 and CARD6

did not require RIP1 kinase activity or the death domain of RIP1. Moreover, CORE-CARD6 was sufficient for interaction with RIP1.

CINCIN1, which contains the CARD and GARR of CARD6 but not the core region, also binds to RICK (4), suggesting that CARD6 can associate with RICK through at least two sites. Indeed, we found that our CARD-GARR(RNR)-CARD6 mutant also bound to RICK. Again, this interaction was compromised if CARD–CARD interactions were not diminished by the RNR mutation (Fig. 1*E*). Unlike RICK, RIP1 bound to both CARD-GARR(RNR)-CARD6 and CARD-GARR-CARD6 (Fig. 1*E* and data not shown).

To determine whether CARD6 could serve as a substrate for RICK or RIP1 *in vitro*, we performed anti-FLAG immune complex kinase assays on precipitates from HEK293T cells expressing either WT-CARD6 or ΔCARD-CARD6 in the presence or absence of RICK, kinase-dead (kd)RICK, or RIP1. No significant RICK kinase activity was pulled down by WT-CARD6 compared with the control reaction containing kdRICK (Fig. 1*F*). Likewise, there was no increase in ^{32}P incorporation into CARD6 in the presence of RIP1 compared with controls lacking RIP1. However, RICK autophosphorylation and ^{32}P incorporation into CARD6 increased significantly if RICK, but not kdRICK, was coimmunoprecipitated with ΔCARD-CARD6. Western blot analysis confirmed that equal levels of RICK, RIP1, and CARD6 variant proteins were present in the immunoprecipitates. Thus, human CARD6 is a RICK- and RIP1-interacting protein and an *in vitro* substrate of either RICK itself or an associated RICK-dependent kinase. Moreover, the CARD of CARD6 impairs the binding of CARD6 to RICK but not to RIP1.

CARD6 Localizes to Microtubules in a CARD- and PRR-Dependent Manner. We speculated that the CARD of CARD6 might indirectly control intermolecular interactions with RICK by specifying posttranslational modifications that determine binding properties and spatial proximity. When examined by immunohistochemistry, human (Fig. 2 *Left*) and mouse (data not shown) WT-CARD6 expressed in COS7 cells colocalized with microtubules, a finding that became more evident if the microtubules were stabilized by paclitaxel treatment (Fig. 9*A Left*, which is published as supporting information on the PNAS web site). Treatment of cells with nocodazole resulted in destruction of the microtubule network and relocalization of WT-CARD6 to the cytosol (Fig. 9*A Right*). Deletion of the CARD6-PRR also abolished colocalization with microtubules, as did loss of the CARD (Fig. 2 *Center* and *Right*). Staining of Huh7 hepatoma cells (which express high levels of endogenous CARD6) with anti-human CARD6 confirmed microtubular localization of the endogenous protein (Fig. 9*B*). These data demonstrate that CARD6 associates with microtubules in a manner that is controlled by the CARD and PRR.

The CARD of RICK Mediates Targeting of CARD6 to Aggresomes. We next examined the influence of RICK and RIP1 on CARD6 localization. Although exogenous RICK accumulated in aggresomes, RIP1 exhibited only diffuse cytoplasmic staining (data not shown). Aggresomes are ubiquitin-rich cytoplasmic inclusions that form around the microtubule-organizing center (MTOC) via microtubule-directed protein transport if the proteasomes are compromised or overwhelmed. Proteins accumulating in aggresomes are sheathed in the intermediate filament protein vimentin (24). Coexpression of RICK with WT-CARD6 induced redistribution of WT-CARD6 from the microtubules into RICK-containing aggresomes (Fig. 3 *Top*). Furthermore, CARD6 protein accumulating at the MTOC in the presence of exogenous RICK was coated in vimentin (Fig. 10*A*, which is published as supporting information on the PNAS web site). In

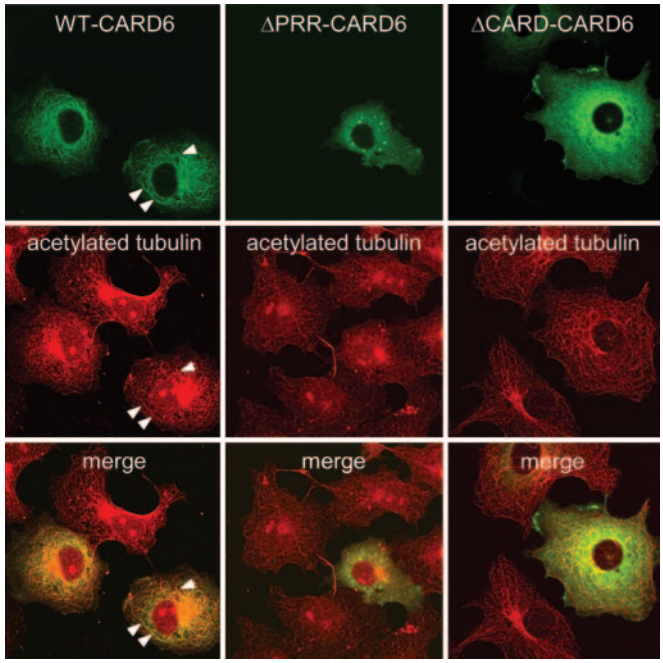

Fig. 2. CARD6 colocalizes with microtubules in a PRR- and CARD-dependent manner. COS-7 cells expressing FLAG-tagged WT-CARD6 (*Left*), ΔPRR-CARD6 (*Center*), or ΔCARD-CARD6 (*Right*) were stained with anti-huCARD6 and anti-acetylated tubulin Abs. Arrowheads point to specific structures to show colocalization of WT-CARD6 with microtubules (*Left*). For all immunohistochemical figures, primary Abs were visualized as described in *Supporting Text*.

contrast to RICK, RIP1 was largely unable to induce WT-CARD6 translocation to aggresomes (Fig. 10*B*). Coexpression of kdRICK with WT-CARD6 demonstrated that RICK kinase activity was not required for targeting WT-CARD6 to aggresomes (data not shown). To test whether the CARD of RICK was required for the translocation of WT-CARD6 to aggresomes, we coexpressed WT-CARD6 and ΔCARD-RICK and performed costaining. As shown in Fig. 3 *Middle*, ΔCARD-RICK was unable to induce WT-CARD6 relocalization. Truncation of CARD6's CARD, which blocked association with microtubules, rescued not only binding to ΔCARD-RICK but also colocalization of both molecules in the cytosol (Fig. 3 *Bottom*). Investigation of the localization of CARD6(RNR) provided evidence that conformational changes in the CARD6-CARD may play a role in aggresomal targeting. CARD6(RNR) exhibited a more diffuse staining pattern than WT-CARD6. Interestingly, in most cells, CARD6(RNR) accumulated in aggresomes (Fig. 10*C*) and colocalized with RICK (Fig. 10*D Upper*). In contrast, ΔCARD-CARD6 and RICK colocalized in the cytosol (Fig. 10*D Bottom*). These results show that the CARDs of CARD6 and RICK control both the colocalization and interaction of these proteins.

CARD6 Positively Modulates NF-κB Activation. To gain more insight into the role of CARD6 in RIP kinase signaling, we analyzed the effect of WT-CARD6 expression on NF-κB activation mediated by various signal transduction pathways. Neither WT-CARD6 (Fig. 4*A*) nor any of the CARD6 truncation mutants (data not shown) induced NF-κB activation when overexpressed in HEK293T cells. Moreover, WT-CARD6 did not contribute significantly to NF-κB activation triggered by TNFα (Fig. 4*A*). However, when WT-CARD6 was coexpressed with NOD1, a synergistic increase (1.5-fold) in NOD1-induced NF-κB activation was observed. A more dramatic 3- to 5-fold increase in NF-κB activation induced by overexpression of RICK, RIP1,

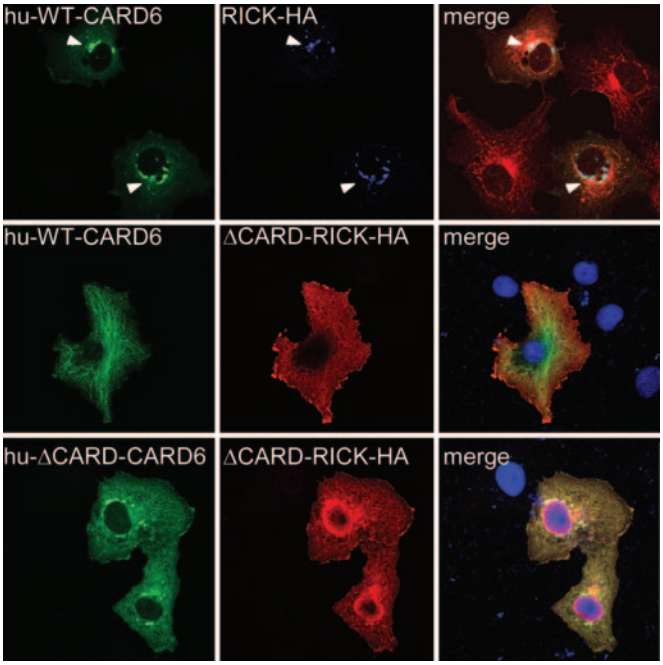

Fig. 3. Coexpression of RICK induces translocation of CARD6 to aggresomes in a CARD-dependent manner. COS-7 cells expressing FLAG-tagged WT-CARD6 and HA-tagged RICK (*Top*) were stained with anti-huCARD6 and anti-HA(3F10) Abs. Cells were counterstained with anti-acetylated tubulin Ab (*Right*). Arrowheads point to areas of aggresome assembly. COS-7 cells cotransfected with FLAG-tagged WT-CARD6 and HA-tagged ΔCARD-RICK (*Middle*) or FLAG-tagged ΔCARD-CARD6 and HA-tagged ΔCARD-RICK (*Bottom*), were stained with anti-huCARD6 and anti-HA(12CA5) Abs. Nuclei were counterstained with DAPI (*Right*). Images showing unmerged counterstains have been excluded.

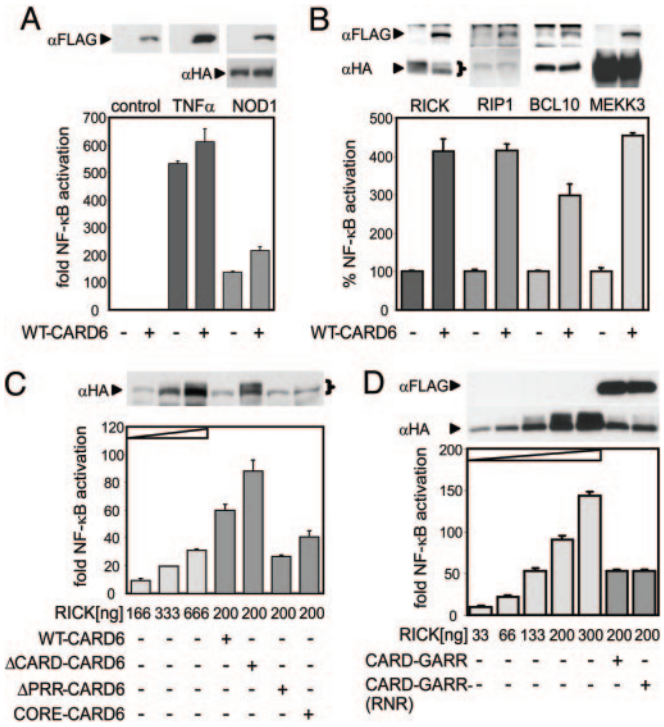

Fig. 4. CARD6 synergistically promotes NF-κB activation. (*A* and *B*) HEK293T cells were transfected with control plasmid or FLAG-tagged human WT-CARD6 and treated with TNFα (*A*) or cotransfected with HA-tagged NOD1 (*A*), or cotransfected with RICK, RIP1, BCL10 or mitogen-activated protein kinase kinase kinase 3 (*B*). Induction of NF-κB activation was determined by using the pBVIx-Luc and pRL-TK luciferase reporter constructs. (*C* and *D*) Cotransfections were with the indicated FLAG-tagged human CARD6 variants plus the indicated amounts of HA-tagged RICK. Induction of NF-κB activation was determined as for *A* and *B*. Because coexpression of ΔCARD-CARD6 leads to an increase in RICK expression (although other variants inhibit expression), the amounts of transfected RICK cDNA were titrated to provide control samples with similar expression levels. Results shown are the means of normalized values ± SD of triplicate cultures. For *A*, *C*, and *D*, results were normalized to values obtained by cotransfection of reporter constructs with empty vectors (1-fold). For *A–D*, expression of transfected constructs was determined by Western blotting with anti-FLAG and anti-HA(3F10) Abs (*Top*). The amount of extract subjected to SDS/PAGE in each case was normalized by Renilla luciferase (pRL-TK) assay.

BCL10, or mitogen-activated protein kinase kinase kinase 3 (MEKK3) occurred if WT-CARD6 was also present (Fig. 4*B*). All CARD6 truncation mutants containing the CARD6-CORE also synergistically enhanced NF-κB activation induced by overexpression of RICK (Fig. 4*C*), RIP1, or BCL10 (data not shown), demonstrating that overexpression of CORE-CARD6 is sufficient for enhancement of NF-κB activation. With respect to other transcription factors, WT-CARD6 did not induce activator protein-1 (AP-1) itself but had a stimulatory effect on MEKK3-induced AP-1 activation (Fig. 11*A*, which is published as supporting information on the PNAS web site). In addition, WT-CARD6 could not induce an IFN regulatory factor 3 (IRF-3) reporter gene (Fig. 11*B*), unlike the positive control melanoma differentiation-associated gene-5 (MDA-5) (25).

It was previously reported that CINCIN1 had a negative effect on NF-κB activation induced by RICK (4). Our CARD-GARR- and CARD-GARR(RNR)-CARD6 mutants did not affect RICK-induced NF-κB activation but did inhibit expression of exogenous RICK protein (Fig. 4*D*). Intriguingly, exogenous CARD6 regulated a covalent modification of RICK that was manifested as a mobility shift. Coexpression of WT-CARD6 inhibited this modification of RICK (Fig. 4*B*, bracket), whereas ΔCARD-CARD6 promoted it (Fig. 4*C*, bracket).

To test whether CARD6 was required for NF-κB activation, we took advantage of the high levels of endogenous CARD6 protein expression in Huh7 cells (Fig. 12*A*, which is published as supporting information on the PNAS web site). We used small interfering RNA (siRNA) to inhibit CARD6 expression in Huh7 cells and monitored NF-κB signaling induced by engagement of TNF receptor 1, IL-1 receptor (IL-1R), TLR4/MD-2, or TLR9. NF-κB activation induced by intracellular peptidoglycan or antigen receptor activation was mimicked by overexpression of NOD1 and BCL10, respectively. Of three siRNAs tested, siRNA1 and siRNA2 both suppressed expression of endogenous CARD6, with siRNA2 being more effective than siRNA1 (Fig. 5*A*). In comparison with control siRNA, inhibition of CARD6 expression with siRNA2 or siRNA1 reduced the level of NF-κB activation achieved in all pathways tested in a dose-dependent manner and also decreased basal NF-κB activity (Fig. 5*B*). Studies in RICK-deficient mice have shown that RICK is involved in antigen-induced BCL10-dependent NF-κB activation in T cells (9, 15). To test whether CARD6-mediated enhancement of BCL10-induced NF-κB activation requires RICK, we coexpressed mouse BCL10 and mouse WT-CARD6 in RICK-deficient mouse embryonic fibroblasts (MEFs). Although the overall induction of NF-κB by BCL10 was decreased in RICK−/− MEFs compared with WT cells, CARD6 enhanced NF-κB activation in both WT and RICK−/− MEFs to the same extent (Fig. 12*B*). This finding suggests that CARD6 acts either downstream of RICK, or in a parallel pathway, that may involve other RIP kinases, to optimize BCL10-induced NF-κB activation. Thus, although CARD6 is not an essential player in any of the signal transduction cascades examined here,

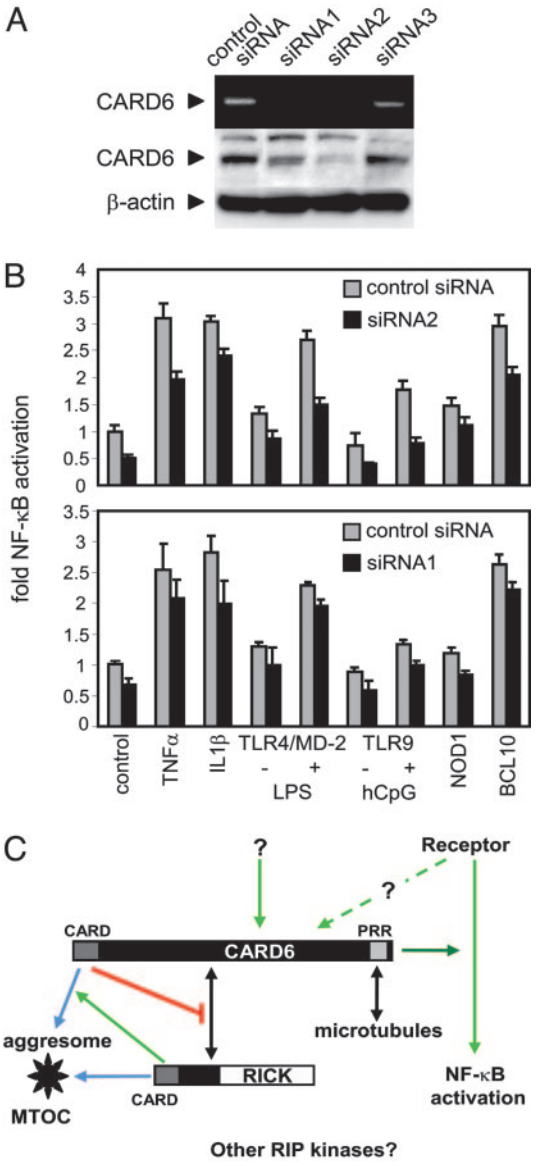

Fig. 5. CARD6 is a general modulator of NF-κB activation pathways. (*A*) RNA interference-mediated suppression of CARD6. Huh7 cells were electroporated with nonsilencing control siRNA or the indicated CARD6-specific siRNAs. At 48 h after electroporation, the relative amounts of CARD6 RNA were determined by using semiquantitative RT-PCR (*Top*). Protein extracts (50 μg) were immunoblotted with anti-hu-CARD6 (*Middle*) or anti-β-actin Abs (*Bottom*). (*B*) Reduction of NF-κB activation by suppression of CARD6. Huh7 cells were electroporated with nonsilencing control siRNA or siRNA2 (*Upper*) or control siRNA or siRNA1 (*Lower*) and transfected 24 h later with empty vector, TLR4/MD-2, TLR9, NOD1, or BCL10 expression constructs in the presence of the pBVIx-Luc and pRL-TK reporters. Triplicate cultures were treated for 4 h with TNF-α, IL-1β, LPS, or hCpG, as indicated, and NF-κB activation was determined as for Fig. 4*A*. Results shown are the means of normalized values ± SD of triplicate cultures. Results were normalized to values obtained by cotransfection of reporter constructs with empty vectors (1-fold) after electroporation of control siRNA. (*C*) Proposed model for CARD6 interactions and function. The PRR of CARD6 is required for its association with the microtubule network. During transient interactions at the microtubules, RICK targets CARD6 to the aggresome in a CARD-dependent manner. Conversely, the CARD6-CARD negatively regulates nonCARD-mediated interactions of CARD6 and RICK. Functionally, CARD6 synergistically enhances NF-κB activation by multiple stimuli via a mechanism that likely requires additional signaling components. Black arrows indicate physical interactions; green arrows and the red connector show positive or negative regulatory mechanisms, respectively; and blue arrows illustrate translocation to the aggresome. (Note: RICK is drawn in reverse orientation.)

our results show that it is an important modulator of NF-κB activation induced by multiple stimuli.

Discussion

The results of this study show that CARD6 is a microtubule-associated protein that forms complexes with RICK (Fig. 5*C*) and RIP1. We have shown there are at least two sites through which CARD6 can associate with RIP kinases. Importantly, we showed that the CARD of CARD6 negatively affected RICK, but not RIP1 binding to CARD6 or its truncation mutants.

CINCIN1 was found to have a negative effect on NF-κB activation induced by RICK and NOD1 (4), the very opposite of the synergistic enhancement exerted by CARD6 in this study. Our results demonstrate that the core region of CARD6 is sufficient for optimization of NF-κB activation, suggesting that the core harbors functional sites necessary for the recruitment of critical signaling components. Stehlik *et al.* (4) have also reported that CINCIN1 is not an *in vitro* substrate of RICK, although they observed CINCIN1 phosphorylation induced by coexpression of either WT or kdRICK. Our data show that ΔCARD-CARD6 is readily phosphorylated either by RICK itself or an associated kinase, that requires RICK kinase activity. These findings indicate that the C terminus of CARD6 harbors additional RICK-dependent phosphorylation sites. Conversely, our analysis has shown that exogenous CARD6 controls a covalent modification of RICK that results in a mobility shift detectable under reducing conditions by Western blotting. Characterization and mutational analysis of these modifications may help to further elucidate CARD6 function.

Our immunohistochemical data demonstrate that WT-CARD6 colocalizes with microtubules. In agreement with our finding that the PRR is required for microtubular colocalization of CARD6, CINCIN1 is not recruited to these structures (4). Interestingly, coexpression of WT-RICK, but not ΔCARD-RICK, with human CARD6 induces translocation of CARD6 from microtubules into aggresomes. We speculate that coexpression of RICK and CARD6 initiates a transient interaction that is followed by covalent modifications, and that these events ultimately lead to the colocalization of these molecules in aggresomes. Conformational changes in the CARD6-CARD may cause the translocation of CARD6 to the microtubule-organizing center (MTOC), because a mutation in the CARD is sufficient to induce accumulation of CARD6 in aggresomes. A CARD6-CARD-regulated modification of RICK, or inhibition of CARD6 accessibility, may in turn be responsible for negative feedback regulation of CARD6-RICK binding. Our finding that WT-CARD6 (unlike ΔCARD-CARD6) does not interact with ΔCARD-RICK, a RICK truncation mutant that does not induce CARD6 translocation to aggresomes, suggests that aggresomal targeting of CARD6 and inhibition of CARD6-RICK binding are two separate events. Alternatively, the RICK-CARD may be required for the initiation of WT-CARD6–RICK interaction. Taken together, these observations suggest that CARD6 may be involved in microtubular transport mechanisms. Accordingly, proteins that interact with CARD6 may be targeted to the MTOC, resulting in either their inactivation or translocation to a site where they can exert their functions. Conversely, the association of CARD6 with microtubules may be an event of sequestration from NF-κB signals or may support the formation of larger microtubule-associated signaling complexes.

Human CARD6 contains a lengthy sequence related to URG4, a growth and survival factor up-regulated in response to Hepatitis Bx antigen (HBxAG) overexpression (23). HBxAg is a transactivating protein that may contribute to the high risk of hepatocellular carcinoma development among hepatitis B virus carriers (26). It remains to be elucidated whether CARD6 and URG4 act in a common survival pathway. We have shown that a CARD6-dependent pathway contributes to the elevated basal

NF-κB activity of Huh7 hepatoma cells, and that suppression of CARD6 protein expression partially inhibits basal NF-κB activity as well as NF-κB activation induced by a range of stimuli. However, CARD6 is not directly involved in NF-κB signaling cascades triggered by BCL10 or NOD1 overexpression or by engagement of TNF receptor 1, IL-1 receptor, TLR4/MD-2, or TLR9. Because it is not clear what factors determine basal NF-κB activity in a given cell type, it will be interesting to identify the CARD6-containing signaling complexes that determine basal NF-κB activity and fine tune NF-κB-mediated responses in Huh7 cells. Studies of CARD6 mutant mice are needed to dissect the roles and interaction of endogenous CARD6 and RICK in additional signaling networks regulating cell survival and innate or adaptive immune responses. Our study may lead to means of manipulating cellular responses that depend on these pathways.

Materials and Methods

Northern Blotting and RT-PCR. Human and mouse poly(A)+ RNA tissue blots (CLONTECH) were subjected to Northern hybridization according to the manufacturer's instructions. For RT-PCR, 1 μg of RNA was incubated with Reverse Transcriptase Superscript 3 (Invitrogen) and a specific antisense primer according to the manufacturer's protocol. For probes, PCR conditions, and primer sequences, please see *Supporting Text*.

Immunoprecipitations, Western Blotting, and Kinase Assays. HEK293T cells were harvested 36 h after transfection and lysed in 0.2% Nonidet P-40 lysis buffer (50 mM Tris-HCl, pH 7.5/120 mM NaCl/25 mM NaF/40 mM β-glycerophosphate/1 mM sodium vanadate/1 mM benzamidine/1 μg/ml aprotinin/1 μg/ml leupeptin/0.2 mM PMSF/0.2% Nonidet P-40). Proteins were immunoprecipitated by combining soluble cell lysate (0.2–1 mg of protein) with protein G Sepharose 4B (Sigma) coupled to the indicated Abs. After 4 h incubation at 4°C with constant rotation, immunoprecipitates were washed four times with lysis buffer and suspended in SDS/PAGE loading buffer. Immunoprecipitations and Western blot analysis were performed by using the Abs described in *Supporting Text*. For RICK and RIP1 kinase assays, immunoprecipitates were washed four times with lysis buffer and once with kinase buffer (20 mM Hepes, pH 7.4/10 mM $MgCl_2$/10 mM $MnCl_2$). Kinase assays were performed in kinase buffer in the presence of 10 μCi (1 Ci = 37 TBq) [γ^{32}P]ATP/5 μM cold ATP. Reactions were incubated at 30°C for 30 min, stopped by addition of SDS/PAGE loading buffer, and subjected to SDS/PAGE and Western blotting.

Immunohistochemistry. Exponentially growing COS7 cells were plated on coverslips, transfected after 24 h, and processed for indirect immunofluorescence microscopy 48 h after seeding as described in *Supporting Text*. Tubulin stability was manipulated with 10 μM nocodazole or 10 μM paclitaxel (both from Sigma). Images were obtained with either a Zeiss LSM510 or a Zeiss LSM510 META confocal laser scanning microscope equipped with a tunable 2-photon laser.

Luciferase Assays. Cells were plated in six-well culture dishes and transfected with a total of 2 μg of expression constructs in the presence of 200 ng of pBVIx-Luc, activator protein 1 (AP-1)-Luc (Stratagene) or IFN regulatory factor 3 (IRF-3)-Luc reporter plus 200 ng of pRL-TK (Promega) by using the FUGENE 6 transfection reagent (Roche Applied Science). NF-κB, IRF-3, or AP-1 activation was assessed at 24-h posttransfection by using a dual luciferase kit (Promega) according to the manufacturer's instructions. Where indicated, for 4 h before lysis, cells were treated with 20 ng/ml recombinant human TNF-α (BioSource International, Camarillo, CA, PHC3015)/10 ng/ml recombinant human IL-1β (BioSource International, PHC0814)/200 ng/ml LPS (Sigma, L3012), or 5 μM phosphorothioate-modified (x) hCpG (T<u>CG</u>x,T<u>CG</u>x,TTT,TGT,<u>CG</u>xT,TTT,GT<u>C,G</u>xTT) (ACGT, Toronto).

RNA Interference. High-performance purity siRNA duplexes composed of 21 nucleotide sense and antisense strands were synthesized by Qiagen (Valencia, CA) and are described in *Supporting Text*. Huh7 cells were electroporated with 200 pmol of control (nonsilencing) siRNA from Qiagen (80–11310) or CARD6-specific siRNAs, as described (27). Electroporated cells were plated in six-well culture dishes at subconfluent levels, transfected with expression vectors 24 h later, and lysed at 48 h after electroporation.

We thank R. A. Flavell (Howard Hughes Medical Institute, Yale University School of Medicine, New Haven, CT) for RICK−/− mouse embryonic fibroblasts; R. J. Ulevitch (The Scripps Research Institute, La Jolla, CA), G. Núñez (University of Michigan Medical School, Ann Arbor, MI), W.-C. Yeh (Ontario Cancer Institute, Toronto), and J. Ruland (Technical University of Munich, Munich) for plasmids; and M. Saunders for scientific editing. This work was supported by the Terry Fox Program of the National Cancer Institute of Canada (to T.W.M.) and by fellowships from the Cancer Research Institute, New York (to A.D.) and the National Cancer Institute of Canada (to S.P.).

1. Ghosh, S. & Karin, M. (2002) *Cell* **109** Suppl, S81–S96.
2. Bouchier-Hayes, L. & Martin, S. J. (2002) *EMBO Rep.* **3,** 616–621.
3. Weber, C. H. & Vincenz, C. (2001) *Trends Biochem. Sci.* **26,** 475–481.
4. Stehlik, C., Hayashi, H., Pio, F., Godzik, A. & Reed, J. C. (2003) *J. Biol. Chem.* **278,** 31941–31949.
5. McCarthy, J. V., Ni, J. & Dixit, V. M. (1998) *J. Biol. Chem.* **273,** 16968–16975.
6. Inohara, N., del Peso, L., Koseki, T., Chen, S. & Nunez, G. (1998) *J. Biol. Chem.* **273,** 12296–12300.
7. Thome, M., Hofmann, K., Burns, K., Martinon, F., Bodmer, J. L., Mattmann, C. & Tschopp, J. (1998) *Curr. Biol.* **8,** 885–888.
8. Inohara, N., Koseki, T., del Peso, L., Hu, Y., Yee, C., Chen, S., Carrio, R., Merino, J., Liu, D., Ni, J. & Nunez, G. (1999) *J. Biol. Chem.* **274,** 14560–14567.
9. Kobayashi, K., Inohara, N., Hernandez, L. D., Galan, J. E., Nunez, G., Janeway, C. A., Medzhitov, R. & Flavell, R. A. (2002) *Nature* **416,** 194–199.
10. Chin, A. I., Dempsey, P. W., Bruhn, K., Miller, J. F., Xu, Y. & Cheng, G. (2002) *Nature* **416,** 190–194.
11. Girardin, S. E., Boneca, I. G., Carneiro, L. A., Antignac, A., Jehanno, M., Viala, J., Tedin, K., Taha, M. K., Labigne, A., Zahringer, U., *et al.* (2003) *Science* **300,** 1584–1587.
12. Girardin, S. E., Boneca, I. G., Viala, J., Chamaillard, M., Labigne, A., Thomas, G., Philpott, D. J. & Sansonetti, P. J. (2003) *J. Biol. Chem.* **278,** 8869–8872.
13. Inohara, N., Ogura, Y., Fontalba, A., Gutierrez, O., Pons, F., Crespo, J., Fukase, K., Inamura, S., Kusumoto, S., Hashimoto, M., *et al.* (2003) *J. Biol. Chem.* **278,** 5509–5512.
14. Chamaillard, M., Hashimoto, M., Horie, Y., Masumoto, J., Qiu, S., Saab, L., Ogura, Y., Kawasaki, A., Fukase, K., Kusumoto, S., *et al.* (2003) *Nat. Immunol.* **4,** 702–707.
15. Ruefli-Brasse, A. A., Lee, W. P., Hurst, S. & Dixit, V. M. (2004) *J. Biol. Chem.* **279,** 1570–1574.
16. Meylan, E. & Tschopp, J. (2005) *Trends Biochem. Sci.* **30,** 151–159.
17. Hur, G. M., Lewis, J., Yang, Q., Lin, Y., Nakano, H., Nedospasov, S. & Liu, Z. G. (2003) *Genes Dev.* **17,** 873–882.
18. Hsu, H., Huang, J., Shu, H. B., Baichwal, V. & Goeddel, D. V. (1996) *Immunity* **4,** 387–396.
19. Kelliher, M. A., Grimm, S., Ishida, Y., Kuo, F., Stanger, B. Z. & Leder, P. (1998) *Immunity* **8,** 297–303.
20. Meylan, E., Burns, K., Hofmann, K., Blancheteau, V., Martinon, F., Kelliher, M. & Tschopp, J. (2004) *Nat. Immunol.* **5,** 503–507.
21. Balachandran, S., Thomas, E. & Barber, G. N. (2004) *Nature* **432,** 401–405.
22. Koseki, T., Inohara, N., Chen, S. & Nunez, G. (1998) *Proc. Natl. Acad. Sci. USA* **95,** 5156–5160.
23. Tufan, N. L., Lian, Z., Liu, J., Pan, J., Arbuthnot, P., Kew, M., Clayton, M. M., Zhu, M. & Feitelson, M. A. (2002) *Neoplasia* **4,** 355–368.
24. Johnston, J. A., Ward, C. L. & Kopito, R. R. (1998) *J. Cell Biol.* **143,** 1883–1898.
25. Kawai, T., Takahashi, K., Sato, S., Coban, C., Kumar, H., Kato, H., Ishii, K. J., Takeuchi, O. & Akira, S. (2005) *Nat. Immunol.* **6,** 981–988.
26. Henkler, F. F. & Koshy, R. (1996) *J. Viral. Hepat.* **3,** 109–121.
27. Lohmann, V., Korner, F., Dobierzewska, A. & Bartenschlager, R. (2001) *J. Virol.* **75,** 1437–1449.